DOI: 10.1002/chem.200501636

Structures and Electronic Absorption Spectra of a Recently Synthesised Class of Photodynamic Therapy Agents

Angelo Domenico Quartarolo, Nino Russo,* and Emilia Sicilia[a]

Abstract: A theoretical study was performed on a novel class of boron-containing molecules (various substituted tetraarylazadipyrromethenes), which show in vitro activity for application in photodynamic therapy. Geometric optimisation of the structures for the singlet and triplet electronic states was carried out on compounds in vacuo at the density functional level of theory, by employing the PBE0 hybrid functional and the split-valence plus polarisation basis set. The absorbance properties in the UV-visible region were examined by means of time-dependent density functional response theory, using the same functional as mentioned above. To evaluate the influence of the solvent on the excitation energies, the continuum polarisable model was applied. Calculated electronic excitations, such as those regarding the Q-like band, were found to be in good agreement (within 0.01–0.1 eV) with experimental values and experimental trends on changing both the substituents and solvent.

Keywords: density functional calculations · dipyrromethenes · photodynamic therapy · solvent effects · substituent effects

Introduction

Photodynamic therapy (PDT) is a noninvasive, still under investigation, medical technique for the treatment of different types of diseases in oncology and ophthalmology.[1–4] The basic principle of PDT is the combination of a photosensitising drug capable of absorbing within the body's therapeutic window ($\lambda = 620$–850 nm), a light source (e.g., a laser) of an appropriate wavelength and molecular oxygen. The photosensitiser, which accumulates preferentially in cancer cells and has a low dark toxicity, is injected into human body tissue and then irradiated with visible light. After irradiation, the light-activated molecule undergoes different reactions and can decay from a singlet to a triplet excited state, through a radiationless transition (intersystem spin crossing). The rate of the latter step is enhanced by the presence of an atom with a high atomic number (heavy-atom effect) in the molecule. The key cytotoxic agent is singlet molecular oxygen $^1O_2$ ($^1\Delta_g$), which is generated by an energy-transfer reaction from the photosensitiser triplet state to the ground-state molecular oxygen $^3O_2$ ($^3\Sigma_g$).[5] The photosensitiser triplet-state energy should match, for an efficient process, the first excitation energy of molecular oxygen, that is 0.98 eV ($\lambda = 1300$ nm). Photosensitisers currently approved for clinical use belong to various groups. Photofrin, a derivative of hematoporphyrin, was the first and is actually the most used PDT agent for the treatment of stomach, early-stage cervical and skin cancers.[6,7] Other classes of polypyrrole macrocyclic compounds, belonging to the so-called second-generation photosensitisers, such as tin etiopurpurin (Purlytin)[8] or Lutetium texaphyrin (Lutex),[9] are in different stages of clinical trials. On the other hand, non-porphyrin PDT agents such as methylene blue[10] or chalcogenopyrilium compounds[11] have shown only a limited application in PDT due to their dark toxicity and low wavelength absorption ($\lambda <$ 650 nm). Methylene blue, a cationic dye, is applied ex vivo for the inactivation of extracellular enveloped viruses in blood plasma.[7,12]

In the continued effort to design, synthesise and characterise new photosensitisers that exhibit a high efficiency and a low dark toxicity, information from modern theoretical methods is very useful. Indeed, the a priori knowledge of a series of properties (e.g., absorption band, singlet–triplet energy gap, thermodynamic stability, substituent effects, etc.) can be considered a basic requirement before proceeding to the synthesis, chemical-physical characterisation and in vitro and in vivo tests. For example, compounds that show absorption properties in the red part of the therapeutic window, and for this reason can be considered to be good

[a] Dr. A. D. Quartarolo, Prof. N. Russo, Prof. E. Sicilia
Dipartimento di Chimica and Centro di Calcolo ad Alte Prestazioni per Elaborazioni Parallele e Distribuite-Centro d'Eccellenza MURST
Università della Calabria, 87030 Arcavacata di Rende (Italy)
Fax: (+39) 0984-492-044
E-mail: nrusso@unical.it

candidates for application in PDT, in practice can be inefficient if the singlet–triplet energy gap is lower than the energy required to produce $^1O_2$. The theoretical work presented here focusses on the structural, energetic and spectroscopic behaviour of a novel class of non-porphyrin molecules, that is, BF_2-chelated tetraarylazadipyrromethenes, that have been recently synthesised and tested in vitro for use in PDT.[13,14] In particular, we have determined 1) the geometric structures and the conformational behaviour, 2) the absorption spectra and their electronic origin, 3) the singlet–triplet energy gap, 4) the influence of the substituents on the absorption spectra, and 5) the solvent effects. Density functional theory (DFT) and its time-dependent extension (TD-DFT)[15] were used for this purpose.

Computational Methods

All calculations were carried out by using the Gaussian 03 package.[16] Geometry optimisations and frequency calculations for all the studied systems were performed at the density functional level of theory, by employing the PBE0[17,18] hybrid functional, based on the generalised gradient functional proposed by Perdew, Burke and Ernzerhof (PBE)[19] with 25% of exact exchange, in combination with split-valence basis sets augmented with polarisation functions (SVP).[20,21] No symmetry constraints were imposed during the geometry optimisations. Restricted formalism was applied for the singlet electronic states and unrestricted formalism for the triplet states. Absorption spectra were computed as vertical electronic excitations from the minima of the ground-state structures by using time-dependent density functional response theory[22] as implemented in the Gaussian 03 code.[23,24] The TD-DFT calculations were carried out by using the standard 6-31+G* basis sets[25,26] and the same PBE0 exchange-correlation functional that was successfully used previously to reproduce absorption spectra of different molecules, including photosensitisers active in PDT.[27–29] To further verify whether the used basis set was large enough to ensure correct results of excitation energies, we performed TD-DFT computations on compound **1a** (see Figure 1, below) by using basis sets of increasing size. For instance, the first excitation energy, relative to the main absorption band, obtained by employing the 6-31++G**, 6-311+G*, cc-pVDZ and aug-cc-pVDZ basis sets, is 2.13, 2.12, 2.15 and 2.11 eV, respectively. These values agree very well with the 6-31+G* calculation, which gives 2.13 eV at lower computational cost. Moreover, these results agree with the previous studies of Stratmann and Scuseria,[30] Bauernschmitt and Ahlrichs,[31] and Jacquemin et al.,[32] in which the basis-set dependence for excitation energies at the TD-DFT level of theory was carefully investigated. Therefore, the choice of the 6-31+G* basis set seemed to be appropriate.

Solvent effects were evaluated by using the conductor-like approach, in the framework of the polarisable continuum model (PCM),[33,34] because it provides results close to those obtained from the original dielectric model for solvents with high-dielectric constants. Solvent shifts of the excitation bands were obtained by the nonequilibrium implementation of the PCM[35] through single-point calculations on equilibrium geometries, obtained in vacuo.

Results and Discussion

This section is organised into three parts in which the determination of the ground-state geometries, excitation energies and solvent effects will be discussed.

Ground-state geometric structures: The investigated systems, shown in Figure 1, are conformationally characterised by four dihedral angles (φ_1, φ_2, φ_3, φ_4), which define the orientation of the four phenyl rings relative to the central part

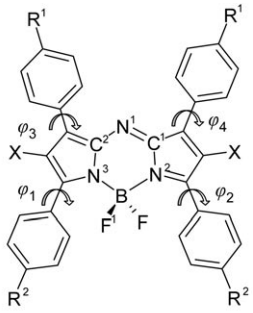

1a: R^1 = H, R^2 = H, X = H
1b: R^1 = H, R^2 = MeO, X = H
1c: R^1 = MeO, R^2 = H, X = H
1d: R^1 = Br, R^2 = H, X = H
2a: R^1 = H, R^2 = H, X = Br
2b: R^1 = H, R^2 = MeO, X = Br
2c: R^1 = MeO, R^2 = H, X = Br

Figure 1. The structure of BF_2-chelated tetraarylazadipyrromethenes used in this study, with the atom, substituent and free-rotation torsion angle labelling.

of the molecule. As a starting point for our calculations, we took into account the crystal-structure data available for compounds **1b** and **2a**.[13,14] To investigate the most stable conformer, separate potential energy surface scans of the dihedral angles φ_1 and φ_3, with a 15° step, were performed starting from the optimised crystal structure, for samples both in vacuo and in ethanol. The energy profiles for φ_1 and φ_3 are very similar in vacuo and in solvent, and are characterised by two minima and two maxima. The minima correspond to the out-of-plane positions of the phenyl rings, whereas the highest energy characterises the planar positions. Similar results were obtained for all the studied systems. Optimised geometric structures corresponding to conformational minima are reported in Figure 2. The structures show a C_2 molecular axis passing through boron and the bridging nitrogen N^1, so selected geometric parameters, reported in Table 1, were averaged between these two parts of each compound. As can be seen from Table 1, the bond lengths and valence angles do not change significantly within each series of compounds (**1** and **2**), showing a good agreement with experimental (exptl) data, with a deviation of less than 0.03 Å and 2° for the bond lengths and angles, respectively. For each series, the optimised dihedral angles φ_1 and φ_2 are almost the same, which corresponds to a parallel orientation of the two moieties, with a maximum difference from experimental data of about 10°. The same behaviour was found for dihedral angles φ_3 and φ_4, with the exception of compounds **2a**–**2c**, for which the phenyl rings are oriented differently. Experimental X-ray measurements of these compounds show that antiparallel orientation of the two moieties is preferred. For φ_1 and φ_2 this behaviour can be ascribed to the interaction between fluorine and the phenyl-ring hydrogen atoms. For φ_3 and φ_4, for which this

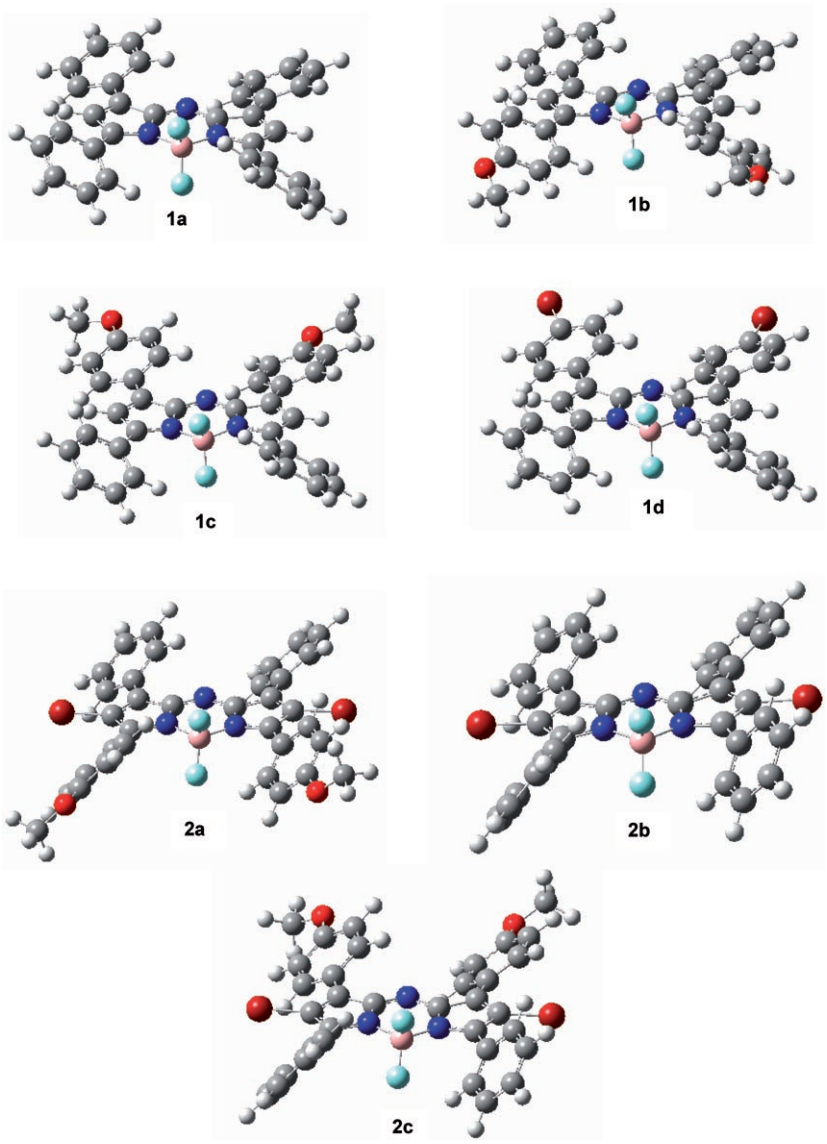

Figure 2. Optimised molecular structures (corresponding to conformational minima) of compounds **1a**–**1d** and **2a**–**2c**.

interaction is absent and the rotation is less hindered in the gas phase, the crystal packing is probably the reason for the discrepancy.

Electronic spectra of compounds in vacuo: The experimental electronic spectra of compounds **1a**–**1d** and **2a**–**2c**,[13] are characterised, in the visible part of the spectrum, by a strong absorbance band ($\approx$0.8 absorbance units) with a sharp profile. Wavelengths corresponding to this maximum range between 1.90 and 1.78 eV, depending on the substituents present (R^1, R^2 and X, see Figure 1) and solvent effects. A secondary band appears at higher energies with a very low intensity ($<$0.2) and a broad character. First, we computed spin-allowed singlet transitions of the compounds in vacuo; the relative results are reported in Tables 2 and 3 for the main excitation energies falling in the visible region, along with their relative oscillator strengths and the transition character. For compounds **1a**–**1d**, the lowest excitation energy gives rise to the more intense transition ($0.7<f<1$) and varies from 2.13 to 2.01 eV. This transition stems mainly from the HOMO$\rightarrow$LUMO excitation (70%)—except for compound **1c** for which there is a small contribution from the HOMO$-$2 to the LUMO (7%)—and corresponds to the strong experimental band that plays the basic role in PDT applications. This can be assigned to a $\pi\rightarrow\pi^*$ transition (Figure 3). The introduction of substituents on the aryl rings (**1b**, **1c**) causes a redshift relative to the "parent" molecule **1a**. In particular, the presence of an electron-donating group in the two isomers **1b** (R^2=MeO) and **1c** (R^1=MeO) causes a shift at lower energy, of 0.12 and 0.10 eV, respectively, with **1b** showing a better conjugation of electronic charge. This effect is less marked for compound **1d**, which has an electron-withdrawing group (R^1=Br), for which the shift is 0.05 eV. A similar trend, owing to the dependence of the lowest excitation energy upon substituents, is shown by the experimental values measured in different solvents. The second excitation energy for **1a**, **1b** and **1d** falls between 2.51 and 2.61 eV and involves electronic transitions from the HOMO$-$2 and HOMO$-$1 to the LUMO with a very weak intensity ($0.003<f<0.017$), so it does not contribute so much to the spectral band appearance. The next excitation energies contribute to the secondary experimental band and vary between 2.43 and 2.73 eV. This contribution is not uniquely defined: for example, in compound **1a** it stems mainly from a HOMO$-$2 to LUMO (89%) excitation with an oscillator strength of 0.273, while for **1b** we obtain a contribution either from the HOMO$-$1 (75%) or the HOMO$-$3 (15%) to the LUMO (f=0.443). In the latter case, we also have an excitation energy at 3.01 eV (f=0.121) that should overlap in the experimental spectrum with the previous transition, corresponding to the secondary band. For compounds **2a**–**2c**, in which bromine atoms are directly bound to the central core of the molecule, there is no significant effect on the lowest excitation energy,

Table 1. Selected geometric parameters for PBE0-optimised geometric structures of compounds **1a**–**1d** and **2a**–**2c**.

	1a	**1b**	**1c**	**1d**	Exptl (**1b**)	**2a**	**2b**	**2c**	Exptl (**2a**)
bond lengths [Å]									
B–F	1.398	1.401	1.399	1.397	1.371	1.391	1.394	1.392	1.376
B–N	1.577	1.574	1.575	1.578	1.562	1.584	1.582	1.582	1.566
N^2–C^1	1.398	1.398	1.398	1.397	1.402	1.396	1.395	1.395	1.394
C^1–N^1	1.325	1.326	1.326	1.326	1.322	1.325	1.325	1.325	1.322
C_{Phenyl}–O	–	1.356	1.358	–	1.372	1.365	1.369	1.366	1.357
C–Br(core)	–	–	–	–	–	1.885	1.887	1.887	1.875
C–Br	–	–	–	1.901	–	–	–	–	–
valence angles [°]									
F^1-B-N^3	111.7	111.8	111.8	111.7	112.0	107.9	107.7	108.0	108.5
B^1-N^2-C1	122.0	121.9	122.1	122.0	122.0	122.7	122.4	122.8	123.2
F-B-F	111.8	111.3	111.6	111.9	110.1	111.6	112.3	112.4	112.6
C^2-N^1-C^1	121.0	120.9	120.9	120.9	119.7	119.5	120.8	120.9	120.9
torsion angles [°]									
ϕ_1	150.1	153.1	149.8	150.0	140.8	45.9	41.5	46.3	50.4
ϕ_2	150.0	153.0	149.8	150.0	144.0	45.9	41.4	46.3	52.6
ϕ_3	156.1	156.3	158.3	156.6	166.3	146.0	145.0	148.9	29.2
ϕ_4	156.2	156.4	158.3	156.6	175.6	146.0	145.6	148.9	131.8

Table 2. Main excitation energies (ΔE), oscillator strengths (f) and transition coefficients computed for compounds **1a**–**1d** in vacuo. All electronic states belong to ^{1}A.

Molecule	Excited state	Transition character	Weight	ΔE [eV]	f
1a	1	HOMO→LUMO	0.580	2.13	0.723
	2	HOMO−1→LUMO	0.668	2.58	0.005
	3	HOMO−2→LUMO	0.667	2.70	0.273
1b	1	HOMO→LUMO	0.583	2.01	0.730
	2	HOMO−2→LUMO	0.668	2.61	0.003
	3	HOMO−3→LUMO	-0.276	2.73	0.443
		HOMO−1→LUMO	0.612		
	4	HOMO−3→LUMO	0.608	3.01	0.121
		HOMO−1→LUMO	0.272		
		HOMO→LUMO+3	0.141		
1c	1	HOMO−2→LUMO	0.191	2.03	0.650
		HOMO→LUMO	0.573		
	2	HOMO−2→LUMO	0.636	2.43	0.113
		HOMO→LUMO	−0.131		
	3	HOMO−1→LUMO	0.665	2.43	0.361
1d	1	HOMO−1→LUMO	−0.111	2.08	0.724
		HOMO→LUMO	0.579		
	2	HOMO−2→LUMO	0.661	2.51	0.017
	3	HOMO−2→LUMO	0.668	2.59	0.350

Table 3. Main excitation energies (ΔE), oscillator strengths (f) and transition coefficients computed for compounds **2a**–**2c** in vacuo. All electronic states belong to ^{1}A.

Molecule	Excited state	Transition character	Weight	ΔE [eV]	f
2a	1	HOMO→LUMO	0.587	2.17	0.722
	2	HOMO−1→LUMO	0.674	2.41	0.000
	3	HOMO−2→LUMO	0.670	2.53	0.194
	4	HOMO−5→LUMO	0.148	3.01	0.002
		HOMO−3→LUMO	0.680		
2b	1	HOMO→LUMO	0.591	2.01	0.733
	2	HOMO−2→LUMO	0.673	2.48	0.003
	3	HOMO−3→LUMO	−0.364	2.59	0.306
		HOMO−1→LUMO	0.565		
	4	HOMO−3→LUMO	0.568	2.78	0.133
		HOMO−1→LUMO	0.364		
2c	1	HOMO−2→LUMO	0.279	2.03	0.506
		HOMO→LUMO	0.557		
	2	HOMO−1→LUMO	0.636	2.30	0.286
	3	HOMO−2→LUMO	0.602	2.30	0.231
		HOMO→LUMO	−0.213		

which ranges from 2.17 to 2.01 eV ($0.5 < f < 0.7$), in comparison with that of **1a**–**1d** (Table 3). Also, in this case we computed a shift to lower energy for **2b** and **2c** of 0.16 and 0.14 eV, respectively, relative to **2a**. In order to relate this behaviour to orbital energies obtained from the geometric optimisation, we sketched correlation energy diagrams (Figure 4) for all of the compounds, reporting the energetic difference between the HOMO and LUMO, which predominantly contributes to the main transition. The trend found is analogous to that found from TD-DFT results: the minimum energetic gap, HOMO→LUMO, along each series is displayed by compounds **1b** and **2b** with values of 2.20 and 2.22 eV (in toluene), respectively. The lower energy transition for **1b** and **2b**, relative to their corresponding isomers, seems to derive from a better energy stabilisation of the HOMO orbital of 0.07 and 0.09 eV, respectively.

Solvent effects: The available experimental absorbance spectra data have been recorded in toluene, chloroform, ethanol, and water containing the emulsifier Cremophor EL.[13] In our work, we exploited the bulk solvation effect on excitation energies, and considered the two very different dielectric media: toluene ($\varepsilon = 2.379$) and ethanol ($\varepsilon = 24.55$). Results for each compound are reported in Table 4 for the lowest excitation energy, together with the corresponding experimental data. As a general remark, we observed a constant shift to lower energies (redshifted wavelengths) relative to the data for the compounds in vacuo. The energetic deviation of the main transition from the experimental data ranges between 0.01 and 0.07 eV, with the exception of compound **2a** whose deviation is about 0.12 eV. So, the introduction of solvent effects improves results by about one order of magnitude with respect to the compounds in vacuo, for which the energetic difference ranges

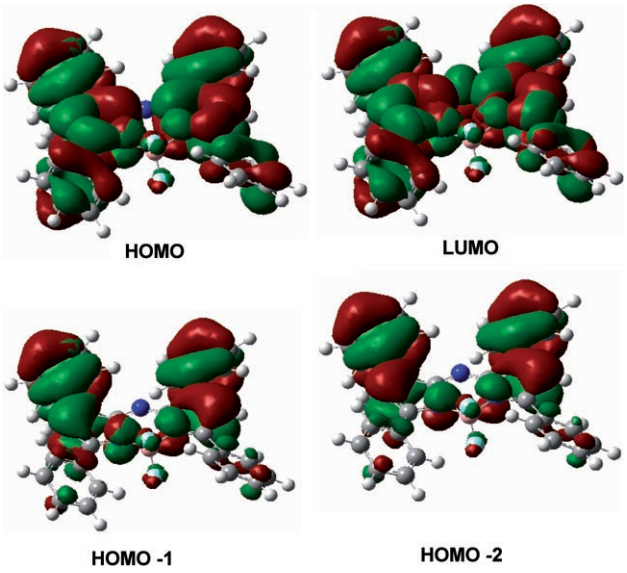

Figure 3. Plot of the HOMO, LUMO, HOMO−1, and HOMO−2 molecular orbitals for compound **1a** in toluene.

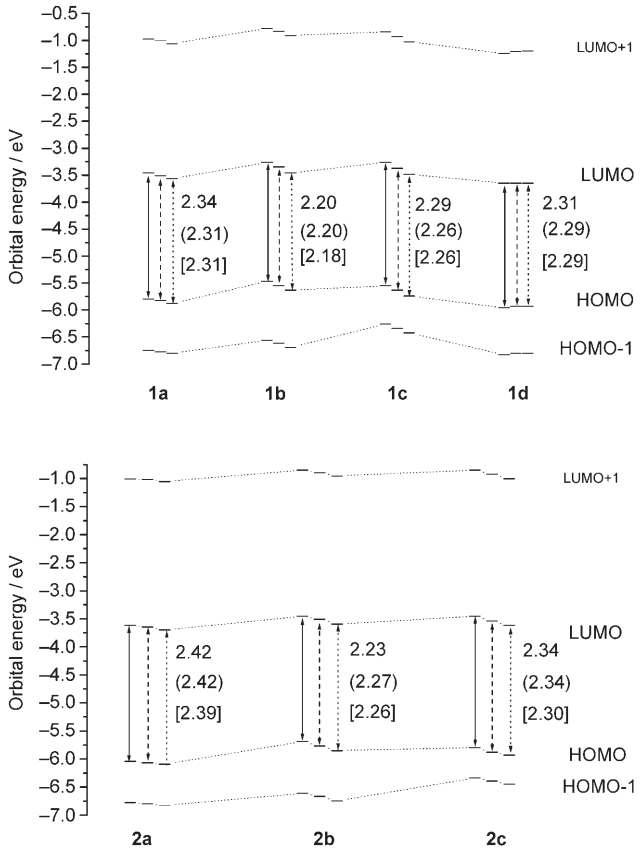

Figure 4. Molecular orbital diagrams of the active orbitals in electronic transitions for **1a**–**1d** (top) and **2a**–**2c** (bottom) in vacuo (solid arrows) and in solvent (dashed arrows = toluene; dotted arrows = ethanol). The HOMO–LUMO gaps are reported for the gas phase, in toluene (values in parentheses) and in ethanol (values in square brackets).

Table 4. Lowest excitation energies (ΔE) and oscillator strengths (f) computed for compounds **1a**–**1d** and **2a**–**2c** in toluene and in ethanol (in parentheses).

Molecule	ΔE [eV]		f		Exptl	
1a	1.96	(1.99)	0.890	(0.853)	1.89	(1.92)
1b	1.84	(1.86)	0.888	(0.853)	1.79	(1.81)
1c	1.87	(1.89)	0.835	(0.779)	1.86	(1.88)
1d	1.92	(1.95)	0.897	(0.862)	1.87	(1.89)
2a	2.00	(2.04)	0.898	(0.859)	1.90	(1.92)
2b	1.85	(1.89)	0.901	(0.865)	1.82	(1.84)
2c	1.90	(1.91)	0.746	(0.681)	1.89	(1.92)

between 0.17 and 0.27 eV relative to the experimental data in toluene. It is worth noting that a slight hypsochromic shift of the main excitation energy is present on going from toluene to ethanol, despite their different polarities. The calculated difference ranges from 0.01 eV for compound **2c** to a maximum of 0.04 eV for compounds **2a** and **2b**. These values are comparable to the experimental difference of about 0.02 eV. The PCM model does not take into account specific interactions that can be present under physiological conditions and that can affect the magnitude of the solvent shift. The studied compounds, owing to their nature, do not present significant specific interactions in solvent so the PCM model is good enough to take into account the main part of the solvent effects, as demonstrated by the good agreement with the experimental data. Also, in the presence of solvent, the excitation energies and the main configuration for the Q-like band derive mainly from the HOMO→LUMO transition (see Figure 3) with increased oscillator strengths with respect to the corresponding values for the compounds in vacuo ($0.681 < f < 0.901$). The role of substituents, in both solvents, is identical to that found in vacuo, with compounds **1b** and **2b** having the lowest excitation energies corresponding to the main transition (1.84 and 1.85 eV in toluene; 1.86 and 1.89 eV in ethanol). A comparison of compounds **1a**–**1c** with their analogues **2a**–**2c** shows lower excitation energy values for the former series by about 0.02–0.04 eV in toluene and 0.02–0.05 eV in ethanol. Therefore, the introduction of bromine atoms does not cause appreciable changes in the absorbance properties. The analysis of the molecular orbitals involved in transitions follows the same trends as the results for the compounds in vacuo. The HOMO→LUMO gap, for both **1a**–**1d** and **2a**–**2c**, does not vary in going from toluene to ethanol, with maximum intensity excitation energies being dependent on the substituent groups on the aryl rings. This gap decreases from **1a** to **1d**, with a minimum for compound **1b** (2.20 eV in toluene); compounds **2a**–**2c** follow the same trend.

Singlet–triplet energy difference: One of the basic requisites of a photosensitiser for achieving an optimal performance in PDT is represented by its singlet–triplet energy gap (greater or equal to 0.98 eV). The PBE0 singlet–triplet energy gaps (ΔE) are reported in Table 5. At first it appears that ΔE is different for the two series of compounds. The first series

Table 5. Total energies and singlet–triplet energetic gaps (ΔE) for the studied compounds in vacuo.

Molecule	Electronic state	Total energy [hartrees]	ΔE [eV]
1a	^{1}A	−1619.8490	–
	^{3}A	−1619.8167	0.87
1b	^{1}A	−1848.6565	–
	^{3}A	−1848.6255	0.79
1c	^{1}A	−1848.6544	–
	^{3}A	−1848.6227	0.86
1d	^{1}A	−6761.4583	
	^{3}A	−6761.4265	0.80
2a	^{1}A	−6761.4502	–
	^{3}A	−6761.4153	0.95
2b	^{1}A	−6990.2567	–
	^{3}A	−6990.2235	0.90
2c	^{1}A	−6990.2562	–
	^{3}A	−6990.2220	0.93

has ΔE values ranging from 0.79 eV (**1b**) to 0.87 eV (**1a**) whereas values equal or higher than 0.90 eV are found for the second series. This means that **2a**–**2c** should induce the triplet–singlet molecular-oxygen transitions. However, it is worth noting that, owing to the small difference in ΔE values, this has to be approached with caution. In fact, compound **1a** is also able to generate singlet oxygen, with a low quantum yield, as found experimentally.[13]

Conclusion

By using the DFT and TD-DFT tools we examined the structural, energetic and UV-visible spectroscopic properties of a new class of photosensitisers recently proposed for their use in photodynamic therapy. Solvent effects were also taken into account. Our results can be summarised as follows: 1) the electronic spectra were correctly reproduced with a good agreement with the experimental data. The origin of the transition has been explained by using frontier molecular orbital diagrams. The main transitions come from HOMO→LUMO excitations with small contributions arising from other neighbouring occupied molecular orbitals; 2) the relationship between the substituent group and the absorption behaviour was shown. As expected, the presence of an electron-donating group causes small redshifts in the spectra; 3) all of the systems show high conformational flexibility of the torsional angles that link the phenyl groups to the core moiety of the molecules; 4) the singlet–triplet energy gap for compounds containing bromine directly bound to the central core of the molecule (**2a**–**2c**) is slightly higher than that found for the corresponding hydrogenated systems, suggesting that, in principle, the former should be more effective as photosensitisers in PDT; 5) the introduction of solvent effects for different media improve the agreement with the experimental data. A slight hypsochromic shift was found for the solvents on going from low to high dielectric constants. We hope that our results can help the experimentalists to develop synthetic strategies for new photosensitisers for use in photodynamic therapy.

Acknowledgements

Financial support from the Università degli Studi della Calabria and Regione Calabria (POR Calabria 2000/2006, misura 3.16, progetto PROSICA) is gratefully acknowledged.

[1] I. J. MacDonald, T. J. Dougherty, *J. Porphyrins Phthalocyanines* **2001**, *5*, 105–129.
[2] Y. Van Tenten, H. J. Schuitmaker, A. De Wolf, B. Willekens, G. F. J. M. Vrensen, M. J. Tassignon, *Exp. Eye Res.* **2001**, *72*, 41–48.
[3] D. E. J. G. J. Dolmans, D. Fukumura, R. K. Jain, *Nat. Rev. Cancer* **2003**, *3*, 380.
[4] T. J. Dougherty, C. J. Gomer, B. W. Henderson, G. Jori, D. Kessel, M. Korbelik, J. Moan, Q. Peng, *J. Natl. Cancer Inst.* **1998**, *90*, 889.
[5] R. Bonnett, *Chem. Soc. Rev.* **1995**, *24*, 19.
[6] D. Wöhrle, A. Hirth, T. Bogdahn-Rai, G. Schnurpfeil, M. Shopova, *Chem. Bull.* **1998**, *47*, 807.
[7] W. M. Sharman, G. M. Allen, J. E. VanLier, *Drug Discovery Today* **1999**, *4*, 507.
[8] T. S. Mang, R. Allison, G. Hewson, W. Snider, R. Moskowitz, *Cancer J. Sci. Am.* **1998**, *4*, 378.
[9] S. W. Young, K. W. Woodbourn, M. Wright, *Photochem. Photobiol.* **1996**, *63*, 892–897.
[10] K. J. Mellish, R. D. Cox, D. I. Vernon, J. Griffiths, S. B. Brown, *Photochem. Photobiol.* **2002**, *75*, 392.
[11] M. R. Detty, P. B. Merkel, *J. Am. Chem. Soc.* **1990**, *112*, 3845.
[12] L. M. Williamson, R. Cardigan, C. V. Prowse, *Transfusion* **2003**, *43*, 1322.
[13] A. Gorman, J. Killoran, C. O'Shea, T. Kenna, W. M. Gallagher, F. D. O'Shea, *J. Am. Chem. Soc.* **2004**, *126*, 10619–10631.
[14] J. Killoran, L. Allen, J. F. Gallagher, W. M. Gallagher, D. F. O'Shea, *Chem. Commun.* **2002**, 1862–1863.
[15] M. Petersilka, U. J. Grossmann, E. K. U. Gross, *Phys. Rev. Lett.* **1996**, *76*, 1212.
[16] Gaussian 03, Revision C.02, M. J. Frisch, G. W. Trucks, H. B. Schlegel, G. E. Scuseria, M. A. Robb, J. R. Cheeseman, J. A. Montgomery, Jr., T. Vreven, K. N. Kudin, J. C. Burant, J. M. Millam, S. S. Iyengar, J. Tomasi, V. Barone, B. Mennucci, M. Cossi, G. Scalmani, N. Rega, G. A. Petersson, H. Nakatsuji, M. Hada, M. Ehara, K. Toyota, R. Fukuda, J. Hasegawa, M. Ishida, T. Nakajima, Y. Honda, O. Kitao, H. Nakai, M. Klene, X. Li, J. E. Knox, H. P. Hratchian, J. B. Cross, V. Bakken, C. Adamo, J. Jaramillo, R. Gomperts, R. E. Stratmann, O. Yazyev, A. J. Austin, R. Cammi, C. Pomelli, J. W. Ochterski, P. Y. Ayala, K. Morokuma, G. A. Voth, P. Salvador, J. J. Dannenberg, V. G. Zakrzewski, S. Dapprich, A. D. Daniels, M. C. Strain, O. Farkas, D. K. Malick, A. D. Rabuck, K. Raghavachari, J. B. Foresman, J. V. Ortiz, Q. Cui, A. G. Baboul, S. Clifford, J. Cioslowski, B. B. Stefanov, G. Liu, A. Liashenko, P. Piskorz, I. Komaromi, R. L. Martin, D. J. Fox, T. Keith, M. A. Al-Laham, C. Y. Peng, A. Nanayakkara, M. Challacombe, P. M. W. Gill, B. Johnson, W. Chen, M. W. Wong, C. Gonzalez, J. A. Pople, Gaussian, Inc., Wallingford CT, **2004**.
[17] M. Ernzerhof, G. E. Scuseria, *J. Chem. Phys.* **1999**, *110*, 5029.
[18] C. Adamo, V. Barone, *J. Chem. Phys.* **1999**, *110*, 6158.
[19] J. P. Perdew, K. Burke, M. Ernzerhof, *Phys. Rev. Lett.* **1996**, *77*, 3865.
[20] A. Schaefer, H. Horn, R. Ahlrichs, *J. Chem. Phys.* **1992**, *97*, 2571.
[21] A. Schaefer, C. Huber, R. Ahlrichs, *J. Chem. Phys.* **1994**, *100*, 5829.
[22] M. E. Casida in *Recent Advances in Density Functional Methods, Part I* (Ed.: D. P. Chong), World Scientific, Singapore, **1995**.
[23] R. E. Stratmann, G. E. Scuseria, M. J. Frisch, *J. Chem. Phys.* **1998**, *109*, 8218.
[24] R. Bauernschmitt, R. Ahlrichs, *Chem. Phys. Lett.* **1996**, *256*, 454.
[25] P. C. Hariharan, J. A. Pople, *Theor. Chim. Acta* **1973**, *28*, 213.
[26] P. M. W. Gill, B. G. Johnson, J. A. Pople, M. J. Frisch, *Chem. Phys. Lett.* **1992**, *197*, 499.
[27] I. Ciofini, C. Daul, C. Adamo, *J. Phys. Chem. A* **2003**, *107*, 11182.
[28] I. Ciofini, P. P. Lainé, F. Bedioui, C. Adamo, *J. Am. Chem. Soc.* **2004**, *126*, 10763.

[29] L. Petit, C. Adamo, N. Russo, *J. Phys. Chem. B* **2005**, *109*, 12214–12221.
[30] R. E. Stratmann, G. E. Scuseria, *J. Chem. Phys.* **1998**, *109*, 8218.
[31] R. Bauernschmitt, R. Ahlrichs, *Chem. Phys. Lett.* **1996**, *256*, 454.
[32] D. Jacquemin, J. Preat, V. Wathelet, M. Fontaine, E. A. Perpete, *J. Am. Chem. Soc.* **2006**, *128*, 2072.
[33] J. Tomasi, M. Persico, *Chem. Rev.* **1994**, *94*, 2027.
[34] V. Barone, M. Cossi, *J. Phys. Chem. A* **1998**, *102*, 1995.
[35] M. Cossi, V. Barone, *J. Chem. Phys.* **2001**, *115*, 4708.

Received: December 29, 2005
Revised: May 4, 2006

Please note: Minor changes have been made to this manuscript since its publication in *Chemistry—A European Journal* Early View. The Editor.

